

Influence of mass difference on dynamic properties of isotope mixtures

N. Kiriushcheva^{1,*} and S.V. Kuzmin¹

¹*Department of Applied Mathematics, University of Western Ontario, London, Ontario N6A 5B7, Canada*

(Dated: November 15, 2018)

We present the results of a Molecular Dynamics computer simulations of a two component isotope mixture of Lennard-Jones particles, monodisperse in size but different in masses, at a fixed average density and temperature. We study changes in properties that result from mass heterogeneity, by measuring the pair distribution function, diffusion coefficient, velocity autocorrelation function, non-Gaussian and isotope effect parameters, as functions of the degree of mass difference. Our results show that if static properties are not influenced by a variation of mass variation, the dynamic properties are significantly affected and even exhibit the presence of “critical” values in the mass difference. We also demonstrate that our model gives a simple contra example to a recently proposed a universal scaling law for atomic diffusion in condensed matter [M. Dzugudov, *Nature*, **381**, 137 (1996)].

PACS numbers: 05.20.Jj, 61.20.Ja, 66.10.-x

I. INTRODUCTION

The aim of this paper is to study, using Molecular Dynamics (MD) computer simulations, the effect of having a mass difference in particles on properties of liquids. The influence of mass polydispersity on dynamical properties when simulating the dynamics of realistic system having size polydispersity was recently demonstrated by Poole and one of the authors (N.K.) [1]. Computer simulation methods, MD in particular, gives unique possibility to isolate and study the role of a single parameter for systems of any complexity that is much more difficult to accomplish (or even impossible) in an actual experiment.

Here we consider a model that allows us to isolate completely the effect of only changing the masses of the particles by keeping all other characteristics of system unchanged. Our model is the simplest possible isotope system: a two-component mixture of isotopes, particles of the same size but different masses, consisting of 50% particles *A* with mass $m_A = m_0 - \Delta m$ and 50% particles *B* with mass $m_B = m_0 + \Delta m$, so that no matter how we change Δm , the average mass of particles, total mass and average mass and number densities of a system remain the same. In this sense, our model differs from these studied previously. For example, Ebbsjö *et al.* in [2] and Bearman and Jolly in [3] studied isotope systems in which one species had a fixed mass and the mass of another species varied. Consequently, this affected the average mass and mass density. Other authors [4, 5, 6, 7, 8] considered the diffusion of solute particles in the limit of infinite dilution in a solvent.

We perform the equilibrium MD simulation of a 3-dimensional system of $N = 4000$ particles interacting via the shifted-force Lennard-Jones (LJ) potential [9], a modification of the standard LJ potential

$$V(r) = 4\varepsilon \left[\left(\frac{\sigma}{r} \right)^{12} - \left(\frac{\sigma}{r} \right)^6 \right], \quad (1)$$

where ε characterizes the strength of the pair interaction and σ describes the particle diameter. Both ε and σ are constant for all particle pairs. In the shifted-force LJ interaction, the LJ potential and force are modified so as to go to zero continuously at $r = 2.5\sigma$, and interactions beyond 2.5σ are ignored. We chose the Lennard-Jones potential because it is very popular in MD studies and

*Electronic address: nkiriusc@uwo.ca

has proved to be a good approximation, for example, for liquid argon. In addition, there is a large amount of data, both theoretical and experimental, available for comparison [10, 11, 12, 13].

In our work we use reduced units. Energy is expressed in units of ε , mass m in units of m_0 , length in units of σ , the number density of particles ρ in units of σ^{-3} , and temperature T in units of ε/k , where k is Boltzmann's constant. Time t is expressed in units of $\sqrt{m_0\sigma^2/\varepsilon}$. In these units the time step used for integrating the particle equations of motion is 0.01. The initial distribution of velocities was Maxwellian.

After equilibration, all quantities are evaluated in the microcanonical ensemble (a constant NVE). We present data for $\rho = 0.75$ and $T = 0.66$ that is not far from a triple point of one component fluid ($\rho_t = 0.85, T_t = 0.76$ [14]) where the cooperative motion of liquid particles is more prominent. We conduct simulations for different Δm from 0 to 0.7 with the step 0.1.

II. PAIR DISTRIBUTION FUNCTION, DIFFUSION COEFFICIENT, AND VELOCITY AUTOCORRELATION FUNCTION

The pair distribution function $g(r)$ that characterizes the average liquid structure [15] is shown in Fig. 1. We calculate $g(r)$ for systems with different values of Δm and for each species A and B of these systems. We find that the pair distribution function $g(r)$ is the same in all cases, confirming that the static properties of the system do not depend on Δm [15].

Fig. 2 presents the dependence of $\langle |\mathbf{r}(t) - \mathbf{r}(0)|^2 \rangle$ (the mean square displacement of a particle) on t for different Δm . As Δm becomes larger, $\langle |\mathbf{r}(t) - \mathbf{r}(0)|^2 \rangle$ has a steeper slope. In addition, in Fig. 3 we plot three graphs that show the mean square displacements of particles A , B , and the total $\langle |\mathbf{r}(t) - \mathbf{r}(0)|^2 \rangle$ for $\Delta m = 0.7$, as an example. The curves for particles with mass $m_A = m_0 - \Delta m$ lie above and for particles with mass $m_B = m_0 + \Delta m$ lie below the curve for the total mean square displacement. This demonstrates the fact that lighter particles not only move faster between collisions, but also diffuse faster than heavier particles. It is interesting that for small t the graph of the mean square displacement of a lighter particle has a steep slope which decreases and becomes constant for $t > 0.15$, whereas the graph of the mean square displacement of a heavier particle increases for $0 < t < 0.15$.

We calculate the diffusion coefficient D in two ways: using the Einstein relation [15]

$$D_E = \lim_{t \rightarrow \infty} \frac{\langle |\mathbf{r}(t) - \mathbf{r}(0)|^2 \rangle}{6t} \quad (2)$$

and using the Kubo formula [15]

$$D_K = \frac{1}{3} \int_0^\infty \langle \mathbf{v}(0) \cdot \mathbf{v}(t) \rangle dt, \quad (3)$$

where $\langle \mathbf{v}(0) \cdot \mathbf{v}(t) \rangle$ is the velocity autocorrelation function. Here and below subscripts E and K mean that D calculated using the Einstein formula and using the Kubo formula.

The results are presented in the Table I. $D_{A(B)}$ is the diffusion coefficient in scaled units for species with mass $m_{A(B)}$, and D is the average diffusion coefficient of the mixture. At fixed ρ and T the diffusion coefficients D , D_A , and D_B increase as Δm increases.

D_E and D_K are equal within the computational uncertainties; however we find that calculations using Eq. (2) are more accurate. The same conclusion was made in Ref. [16]. This is because Eq. (3) involves integration where negative and positive parts of $\langle \mathbf{v}(0) \cdot \mathbf{v}(t) \rangle$ partially cancel out and because of uncertainties in the long-time behavior of the velocity autocorrelation function, whereas the graphs of $\langle |\mathbf{r}(t) - \mathbf{r}(0)|^2 \rangle$ versus t are almost perfect straight lines for $t > 0.15$.

From the Table I we can see that the relationship $D_A > D > D_B$ always holds and the difference among D_A , D , and D_B increases with an increase of Δm . This is shown in Fig. 4. The dependence of the diffusion coefficient versus Δm is not linear.

Even though the diffusion coefficient does not change too much with a change of mass (if Δm changes by 1%, D changes maximum by 5%), the velocity autocorrelation function varies significantly, both in shape and magnitude as a function of t . Fig. 5 shows the dependence on Δm of the normalized velocity autocorrelation function $\psi(t)$ [14]

$$\psi(t) = \frac{\langle \mathbf{v}(0) \cdot \mathbf{v}(t) \rangle}{\langle |\mathbf{v}(0)|^2 \rangle}. \quad (4)$$

It is interesting to observe the behavior of the negative part of $\psi(t)$. The velocity autocorrelation function, basically, is the projection of a particle's velocity at time t on the initial velocity of that particle, averaged over all particles. If $\psi(t)$ becomes negative it means that a particle after a number of collisions, on average, reverses the direction of its motion. As we can see from the graph, all of the functions $\psi(t)$ have a negative part but the minimum of $\psi(t)$ behaves differently. For $\Delta m = 0.1$ and 0.2 , the functions $\psi(t)$ are very close to $\psi(t)$ with $\Delta m = 0$. As Δm increases, the minimum shifts to earlier times. Its magnitude initially decreases, has a maximum at $\Delta m = 0.5$, and starts to increase drastically for $\Delta m \geq 0.5$. To reveal this difference we plot three curves on Fig. 6 which shows the velocity autocorrelation functions of particles A , B , and the total value for $\Delta m = 0.7$. The curve for particles with mass $m_A = m_0 - \Delta m$ has a deeper minimum than the total and the curve for particles with mass $m_B = m_0 + \Delta m$ does not have a negative part at all. For a big difference in the masses m_A and m_B , the heavier particles do not reverse their direction of motion on average, even in a dense fluid.

III. NON-GAUSSIAN AND ISOTOPE EFFECT PARAMETERS

The general non-Gaussian parameter $\alpha_n(t)$ is defined as [14]

$$\alpha_n(t) = \frac{\langle r^{2n}(t) \rangle}{c_n \langle r^2(t) \rangle^n} - 1, \quad (5)$$

where $c_n = [1 \cdot 3 \cdot 5 \cdots (2n + 1)]/3^n$ and $\langle r^{2n}(t) \rangle$ are the ensemble average of the $2n^{th}$ power of the particle displacements after a time t [12]:

$$\langle r^{2n}(t) \rangle = \left\langle \frac{1}{N} \sum_{i=1}^N |\mathbf{r}_i(t) - \mathbf{r}_i(0)|^{2n} \right\rangle. \quad (6)$$

For systems in which motions of particles are uncorrelated (for example, in an ideal gas) $\alpha_n(t) = 0$. The deviation of $\alpha_n(t)$ from zero serves to quantify the correlation of particle motions at intermediate time or, as it was shown in [1], the heterogeneity in masses for short times.

Here, as in [1], we calculate $\alpha_2(t)$:

$$\alpha_2(t) = \frac{3\langle r^4(t) \rangle}{5\langle r^2(t) \rangle^2} - 1. \quad (7)$$

In Fig. 7 we plot $\alpha_2(t)$ for different values of Δm . For small Δm the behavior of $\alpha_2(t)$ is similar to that of a polydisperse system [1]. For $\Delta m \neq 0$, α_2 does not start from 0. We observe the characteristic, intermediate-time peak of α_2 , at approximately $t = 1$, which increases in magnitude as Δm increases. As in [1], the combination of the non-zero, early-time behavior of α_2 , and the intermediate-time peak produces a minimum in α_2 at approximately $t = 0.12$. However, for larger Δm , starting from $\Delta m = 0.5$, the minimum disappears, and $\alpha_2(t)$ becomes a monotonically decreasing function. For these Δm the values of $\alpha_2(t)$ at $t \rightarrow 0$ even exceed the intermediate-time peak. It is interesting to observe how the total non-Gaussian parameter is related to ones of

particles A and B . Fig. 8 shows three curves representing $\alpha_2(t)$ for particles A , B , and the total when $\Delta m = 0.7$. Both curves (A and B) start from 0 (each component has particles of the same size). The curve for particles with mass $m_A = m_0 - \Delta m$ has a maximum that is twice as high and is located at an earlier time than the curve for particles with mass $m_B = m_0 + \Delta m$. The difference between these two curve increases when Δm becomes larger. In addition, the curve for the lighter particle, after passing the maximum, completely coincides with the total $\alpha_2(t)$ and decays as t^{-1} , according to [17]. The lighter particles are more mobile and give a larger contribution to the motion of the fluid.

As we pointed out in [1], the non-Gaussian behavior of $\alpha_2(t)$ shows that the self-part of the van Hove correlation function $G_s(\mathbf{r}, t)$

$$G_s(r, t) = \left\langle \frac{1}{N} \sum_{i=1}^N \delta(r - |\mathbf{r}_i(t) - \mathbf{r}_i(0)|) \right\rangle. \quad (8)$$

deviates from the Gaussian form. In the limit $\mathbf{r}, t \rightarrow 0$, when particles move with a velocity $\mathbf{v}_i = \mathbf{r}_i/t$ as if they were free, this corresponds to the condition that the distribution of velocities of particles is non-Maxwellian. The Maxwell-Boltzmann distribution for particle velocities is [15]

$$\phi_i(v) = \left(\frac{m_i}{2\pi kT} \right)^{3/2} \exp\left(-\frac{m_i |v|^2}{2kT} \right). \quad (9)$$

We can see that it depends on the mass of a particle. Even if for each species the distribution is Maxwellian the total distribution is not

$$\phi_{total}(v) = \frac{N_A}{N} \left(\frac{m_A}{2\pi kT} \right)^{3/2} \exp\left(-\frac{m_A |v|^2}{2kT} \right) + \frac{N_B}{N} \left(\frac{m_B}{2\pi kT} \right)^{3/2} \exp\left(-\frac{m_B |v|^2}{2kT} \right). \quad (10)$$

In Fig. 9 we plot the distribution of velocities of all particles (solid line) and the Gaussian fit of this curve (dashed line). It is clear that this distribution deviates from the Gaussian form. It is narrower and has longer tails for large velocities. This is the contribution of particles with smaller mass. It is interesting that the same non-Gaussian behavior of $G_s(\mathbf{r}, t)$ was observed experimentally in [18] for colloid suspensions. It could be accounted for the polydispersity in the mass of colloids used in that experiment (which was $\sim 8\%$).

Finally, we can use the formula for the non-Gaussian parameter α_2 at $t \rightarrow 0$ for the multicomponent system from [1]:

$$\alpha_2^\circ \equiv \alpha_2(t \rightarrow 0) = \frac{\sum_{i=1}^l n_i/m_i^2}{\left(\sum_{i=1}^l n_i/m_i \right)^2} - 1, \quad (11)$$

where $n_i = N_i/N$ is the fraction of particles of species i . (Here, as in [1], the superscript “o” indicates the limit $t \rightarrow 0$.)

If we have a binary system with two species having masses $m_A = m_0 - \Delta m$ and $m_B = m_0 + \Delta m$, Eq. (11) becomes

$$\alpha_2^\circ = \frac{\frac{n_A}{(m_0 - \Delta m)^2} + \frac{n_B}{(m_0 + \Delta m)^2}}{\left(\frac{n_A}{m_0 - \Delta m} + \frac{n_B}{m_0 + \Delta m} \right)^2} - 1 = \frac{4n_A n_B x^2}{(1 + (n_A - n_B)x)^2}, \quad (12)$$

where $x \equiv \Delta m/m_0$. In our case $n_A = n_B = 1/2$ and

$$\alpha_2^\circ = x^2. \quad (13)$$

We plot α_2° versus Δm in Fig. 10, confirming this analysis.

An additional parameter which could reveal the diffusion mechanism in isotope mixtures is the isotope effect parameter. It was shown by Parrinello *et al.* in [19] that for dilute gases the ratio of the self-diffusion coefficients of a binary mixture is equal to the reciprocal of the square root of masses of the two species. However, computer simulations performed by Bearman and Jolly [3] show that the ratio of the self-diffusion coefficients varies with masses as

$$\frac{D_A}{D_B} = \left(\frac{m_B}{m_A} \right)^\gamma, \quad (14)$$

where γ differs from 1/2 for higher densities and lower temperatures, when effects of collective motion is important. In Fig. 11 we plot $\ln(D_A/D_B)$ versus $\ln(m_B/m_A)$. The slope of the best fit line gives $\gamma = 0.081$. This corresponds to well-known results (for example, therein Ref. [20]). There is another parameter that serves as a quantitative measure of collectivity, the isotope effect, defined as [20]

$$E = \frac{D_A/D_B - 1}{\sqrt{m_B/m_A} - 1}. \quad (15)$$

Large isotope effects are interpreted as single-atom jumps via vacancies [21], whereas small isotope effects indicate the presence of some collective processes. Kluge and Schober in [20] estimated the number of particles moving cooperatively as

$$N \approx \frac{1}{E}. \quad (16)$$

We find that for our binary mixtures the isotope effect E varies from 0.132 for $\Delta m = 0.1$ to 0.109 for $\Delta m = 0.7$. It indicates an increase in the cooperative motion of particles with an increase in their mass differences.

IV. CONCLUSION

We have considered MD computer simulations of a toy model, a binary isotope mixture, that allows us to elucidate the effect of having a mass difference on properties of liquids. It has been shown that redistribution of mass (Δm) among the two species, while keeping the rest of parameters fixed, does not affect static properties (the pair distribution function $g(r)$) both for the system and separately for each species A and B and these are independent of Δm). At the same time, all dynamic properties (the diffusion coefficient, velocity autocorrelation function, non-Gaussian and isotope effect parameters) are affected and exhibit Δm dependence, which demonstrates the pure dynamical nature of mass heterogeneity.

Moreover, the Δm dependence exhibits some “critical” values such as in the behavior of the negative part of the normalized velocity autocorrelation function $\psi(t)$ (see Fig. 5) which at $\Delta m = 0.5$ changes the initial tendency of decreasing magnitude of first minimum with increase of Δm to the opposite, i.e. a drastic increase in $\psi(t)$. Such phenomenon, we believe, deserves further investigation and analysis.

Many real systems have mass heterogeneities but, of course, not pure as in our model. Nevertheless, even the hidden and probably not very strong effect of having a mass difference compared to other (size, interaction, etc.) has to create a pure dynamical contribution. As demonstrated

by our simple model, this pure mass effect does not affect the static properties of a system. In particular, this observation leads us to question the validity of some universal empirical formulae based on the conjecture that “atomic diffusion is an entirely geometrical phenomenon” [22]. The author of [22] claimed that the relationship between D and $g(r)$ is governed by following equations

$$D^* = 0.049e^{S_2}, \quad (17)$$

where D^* is the diffusion coefficient in the dimensionless form $D^* = D\Gamma_E^{-1}\sigma^{-2}$, Γ_E is given by

$$\Gamma_E = 4\sigma^2 g(\sigma)\rho\sqrt{\pi kT/m}, \quad (18)$$

where σ is a position of first maximum of $g(r)$ and S_2 is the two-particle approximation of the reduced excess entropy

$$S_2 = -2\pi\rho \int_0^\infty \{g(r) \ln [g(r)] - [g(r) - 1]\} r^2 dr. \quad (19)$$

According [22], Eqs. (17,18,19) are universal for equilibrium condensed atomic systems, both liquid and solid, regardless of the structures, interatomic interaction potential or the microscopic dynamical mechanisms involved and also valid for multicomponent systems with Γ_E , σ and S_2 corresponding to each type of constituent atoms.

This universality contradicts results of our simulation because Eqs. (17,18,19) for the considered binary mixture give Eq. (14) with $\gamma = 0.5$, whereas from Fig. 11 the slope of the line of best fit gives $\gamma = 0.081$.

For our system the observed difference in the diffusion coefficients of two species is an entirely nongeometrical, nonstatic phenomenon.

V. ACKNOWLEDGMENTS

We thank S. Consta and D.G.C. McKeon for valuable comments and reading the manuscript.

-
- [1] N. Kiriushcheva and P.H. Poole, Phys. Rev. **E 65**, 011402-1 (2002).
 - [2] I. Ebbsjö, P. Schofield, K. Sköld and I. Waller, J. Phys. C: Solid State Phys. **7**, 3891 (1974).
 - [3] R.J. Bearman and D.L. Jolly, Mol. Phys. **44**, 665 (1981).
 - [4] P. Herman and B.J. Alder, J. Chem. Phys. **56** 987 (1972).
 - [5] A.J. Easteal and L.A. Woolf, Chem. Phys. Lett. **167**, 329 (1990).
 - [6] F. Ould-Kaddour and J.-L. Barrat, Phys. Rev. **A 45**, 2308 (1992).
 - [7] M.J. Nuevo, J.J. Morales, and D.M. Heyes, Phys. Rev. **E 51**, 2026 (1995).
 - [8] F. Ould-Kaddour and D. Levesque, Phys. Rev. **E 63**, 011205-1 (2000).
 - [9] M.P. Allen and D.J. Tildesley, *Computer Simulation of Liquids* (Clarendon Press, Oxford, 1987).
 - [10] N.H. March and M.P. Tosi, *Atomic Dynamics in Liquids* (Dover Publications, Inc., New York, 1991).
 - [11] J.J. Nicolas, K.E. Gubbins, W.B. Street and D.J. Tildesley, Mol. Phys. **37**, 1429 (1979).
 - [12] A. Rahman, Phys. Rev. **136**, 405 (1964).
 - [13] J. Naghizadeh and S.A. Rice, J. Chem. Phys. **36**, 2710 (1962).
 - [14] J.P. Boon and S. Yip, *Molecular Hydrodynamics* (Dover Publications, Inc., New York, 1980).
 - [15] J.P. Hansen and I.R. McDonald, *Theory of Simple Liquids* (Academic Press Inc., London, 1986).
 - [16] B. Bernu, J.P. Hansen, Y. Hiwatari, G. Pastore, Phys. Rev. **A 36**, 4891 (1987).
 - [17] T. Yamaguchi and Y. Kimura, J. Chem. Phys. **114**, 3029 (2001).
 - [18] A. Kasper, E. Bartsch, and H. Sillescu, Langmuir **14**, 5004 (1998).
 - [19] M. Parrinello, M.P. Tosi and N.H. March, J. Phys. C: Solid State Phys. **7**, 2577 (1974).

- [20] M. Kluge and H.R. Schober, *Phys. Rev.* **E 62**, 597 (2000).
- [21] V. Zöllmer, H. Ehmler, K. Rätzke, P. Troche and F. Faupel, *Europhys. Lett.* **51**, 75 (2000).
- [22] M. Dzugutov, *Nature* **381**, 137 (1996).

m_A	m_B	$D_{A(E)}$	$D_{A(K)}$	$D_{B(E)}$	$D_{B(K)}$	$D_{(E)}$	$D_{(K)}$
1	1	5.4979	5.4749	5.4979	5.4749	5.4979	5.4749
0.9	1.1	5.5861	5.4866	5.4592	5.7079	5.5355	5.6564
0.8	1.2	5.6677	5.6369	5.4710	5.4368	5.5797	5.4842
0.7	1.3	5.7393	5.7635	5.4802	5.5991	5.6108	5.6169
0.6	1.4	5.9216	5.8336	5.5586	5.5582	5.7045	5.7818
0.5	1.5	6.1117	6.0612	5.5852	5.6850	5.8550	5.9024
0.4	1.6	6.3923	6.6003	5.7286	5.8319	6.0542	6.1483
0.3	1.7	6.7438	6.5358	5.8589	6.0439	6.3819	6.4645

TABLE I: The dependence of the diffusion coefficient on masses of species. All D are multiplied by 10^{-2} (in scaled units).

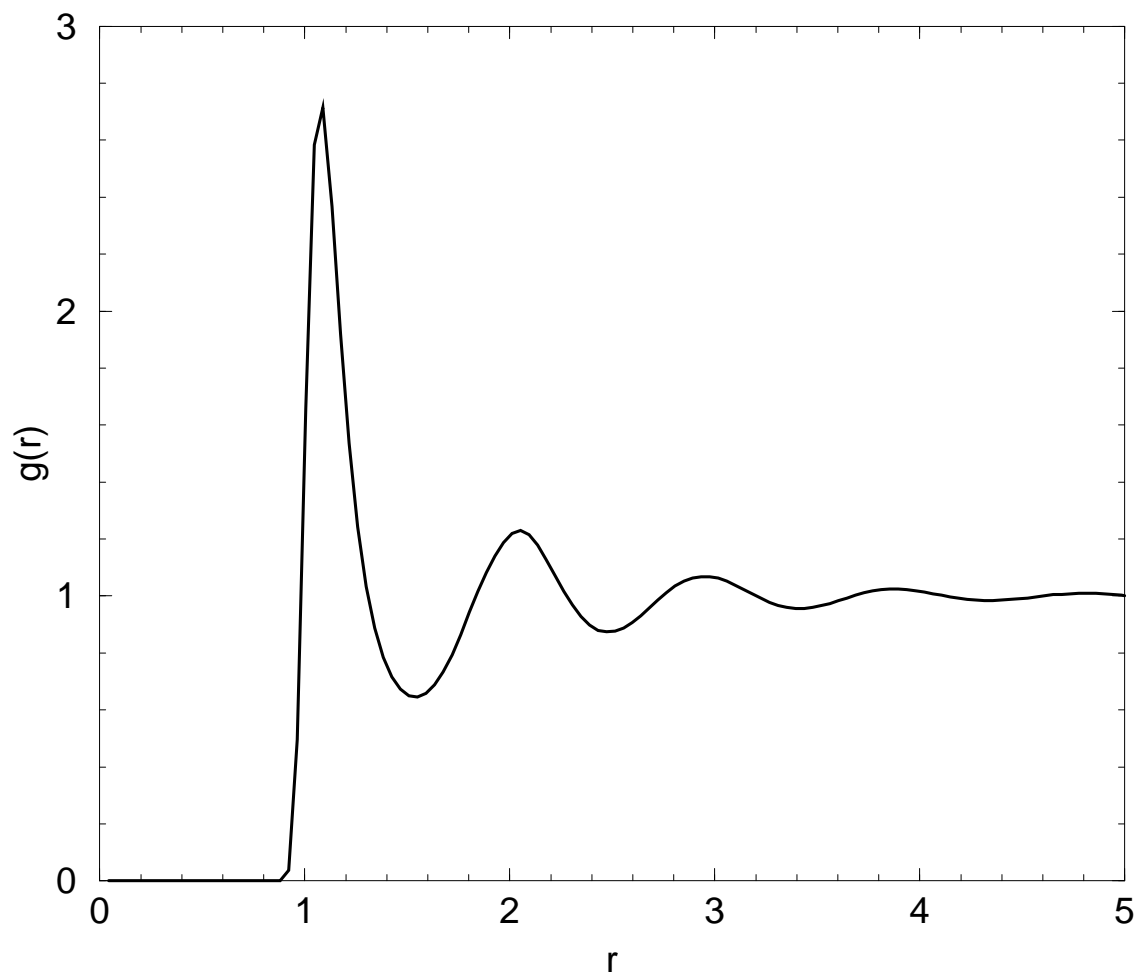


FIG. 1: The pair distribution function $g(r)$ of all species.

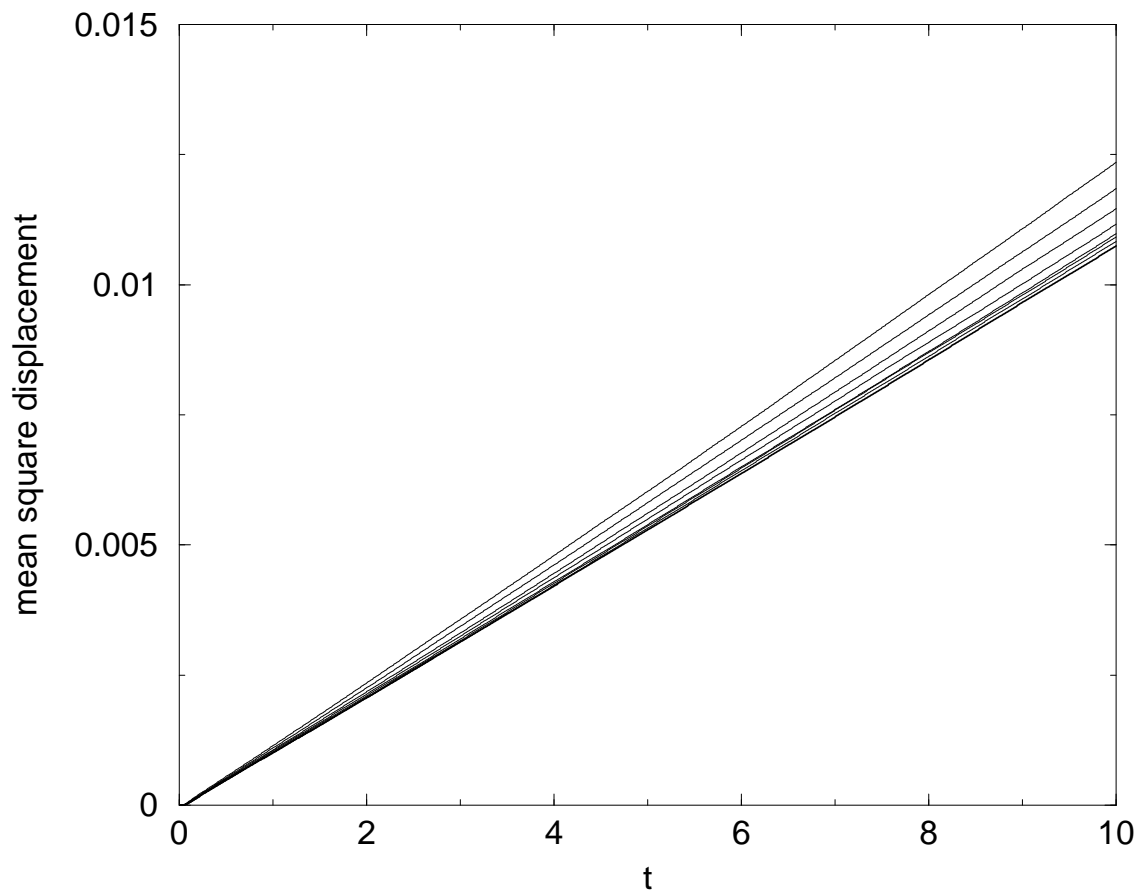


FIG. 2: The mean square displacement versus t for increasing Δm (from the bottom to the top).

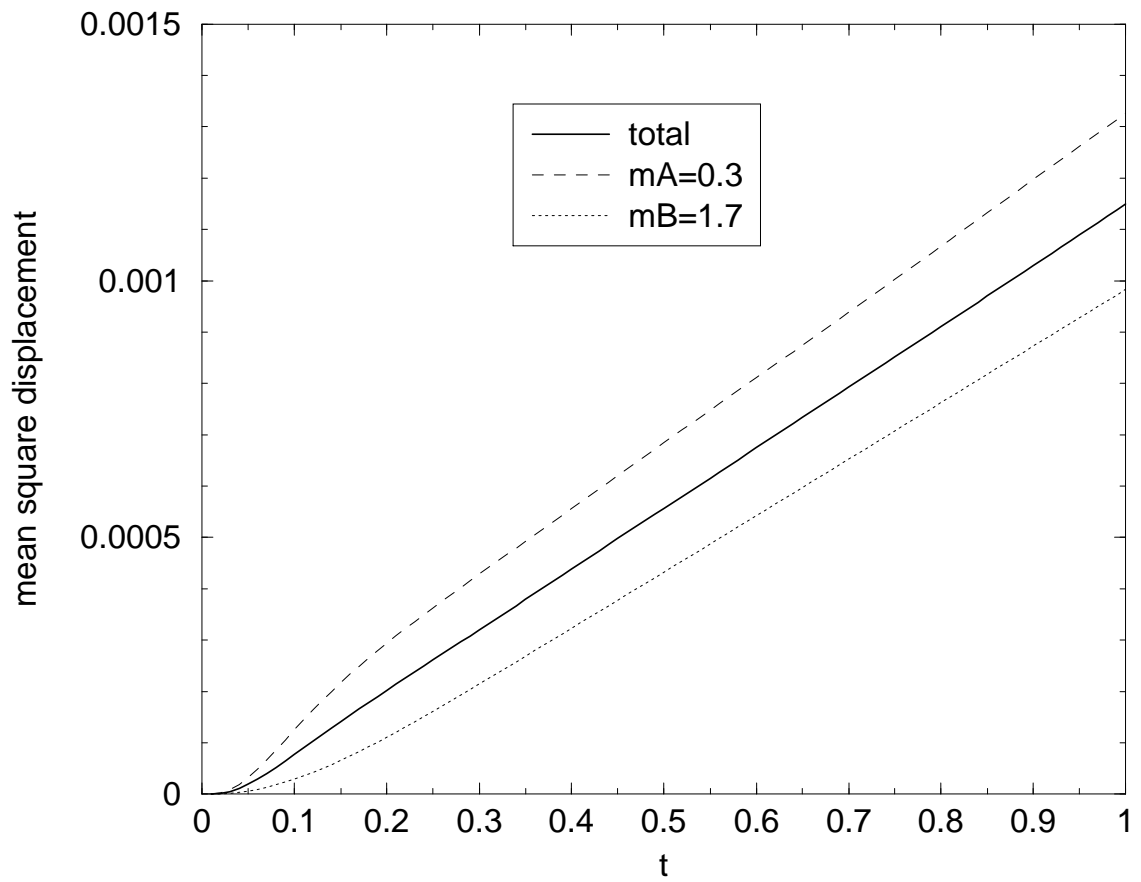


FIG. 3: The mean square displacement versus t for lighter, heavier particles and the total for $\Delta m = 0.7$.

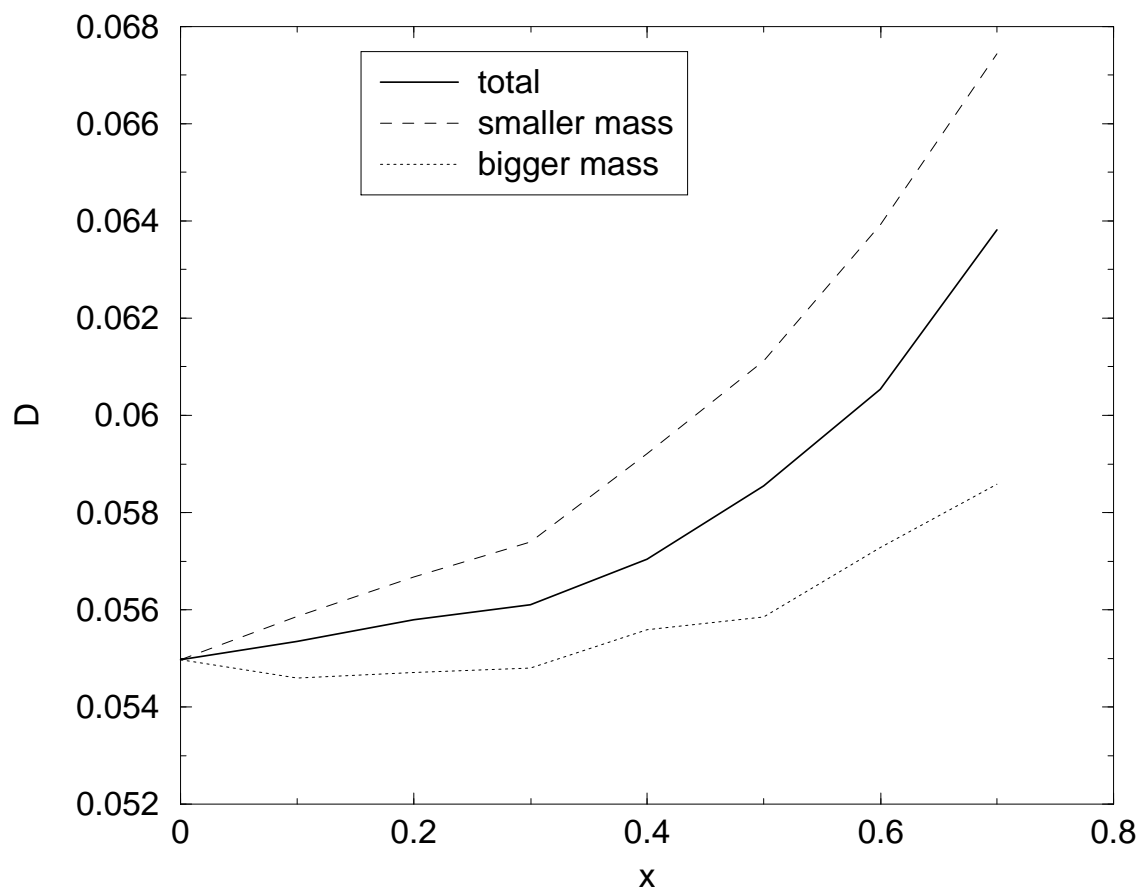


FIG. 4: The diffusion coefficient D versus $x = \Delta m/m_0$ for lighter, heavier particles, and the total.

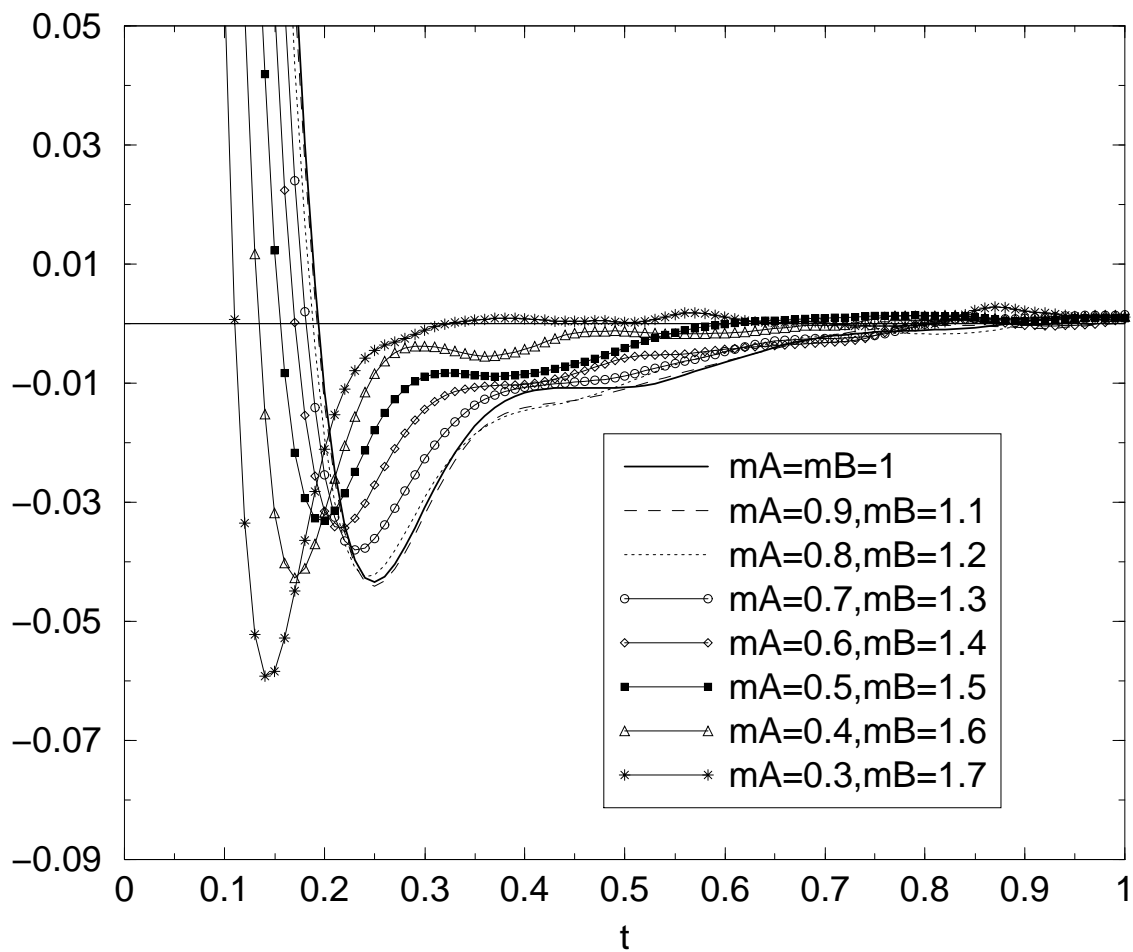


FIG. 5: The velocity autocorrelation function $\psi(t)$ for different Δm .

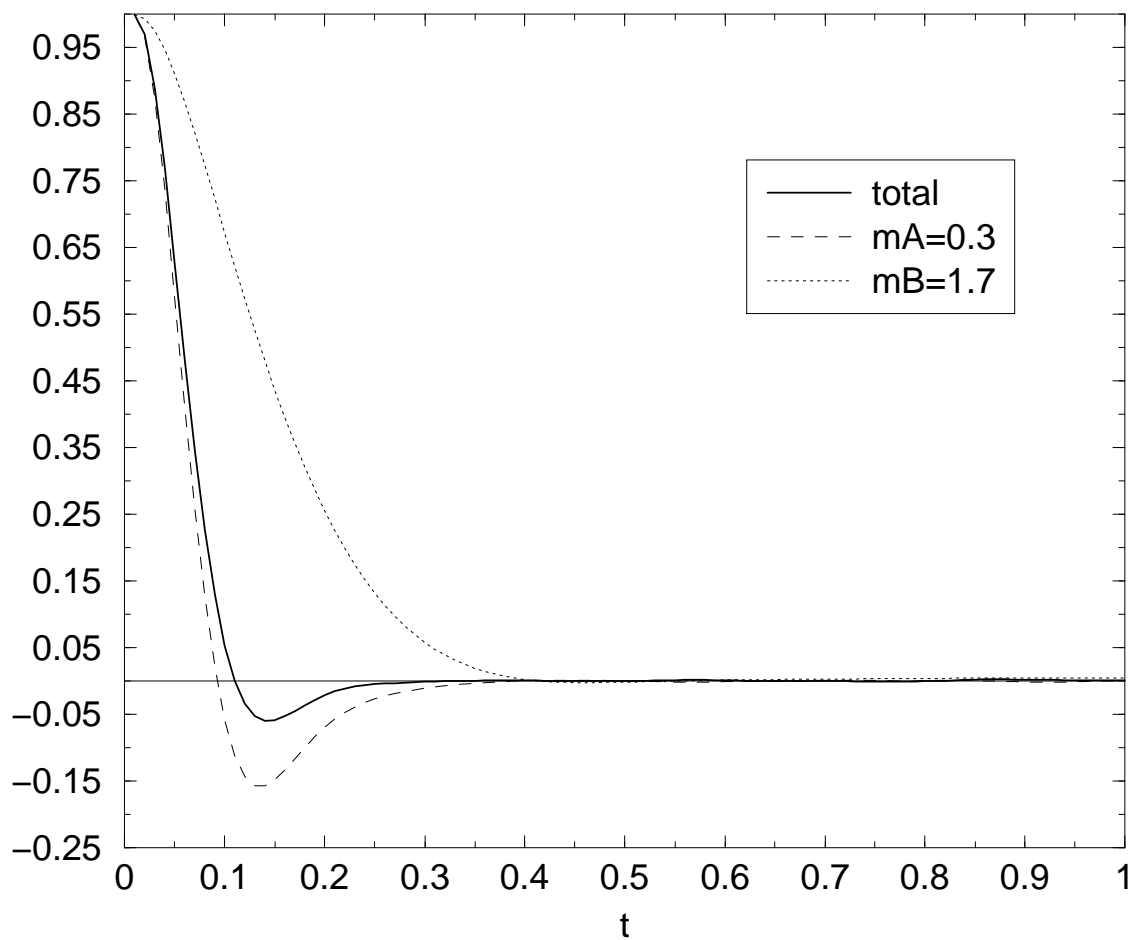


FIG. 6: The velocity autocorrelation function $\psi(t)$ for lighter, heavier particles, and the total for $\Delta m = 0.7$.

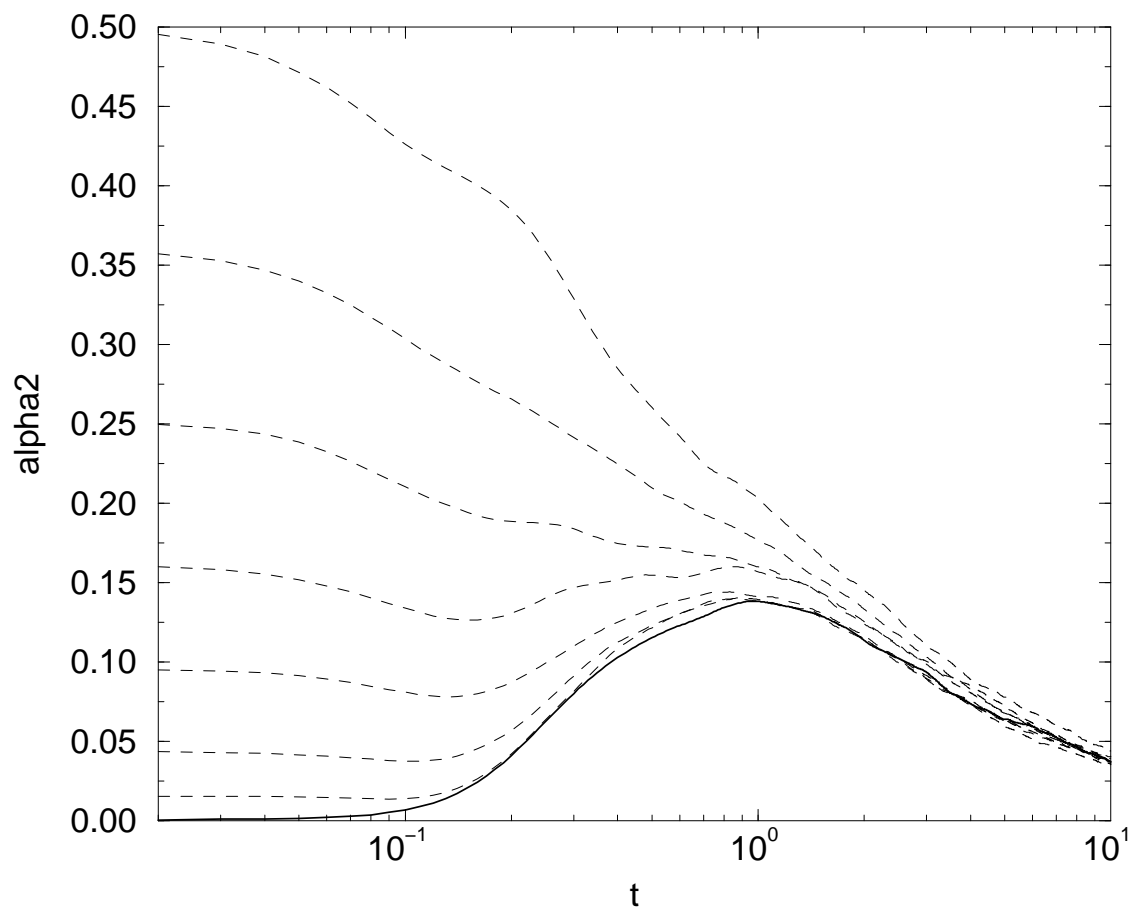


FIG. 7: $\alpha_2(t)$ for $\Delta m = 0, 0.1, \dots, 0.7$ (from the bottom to the top). α_2° increases with increase of Δm .

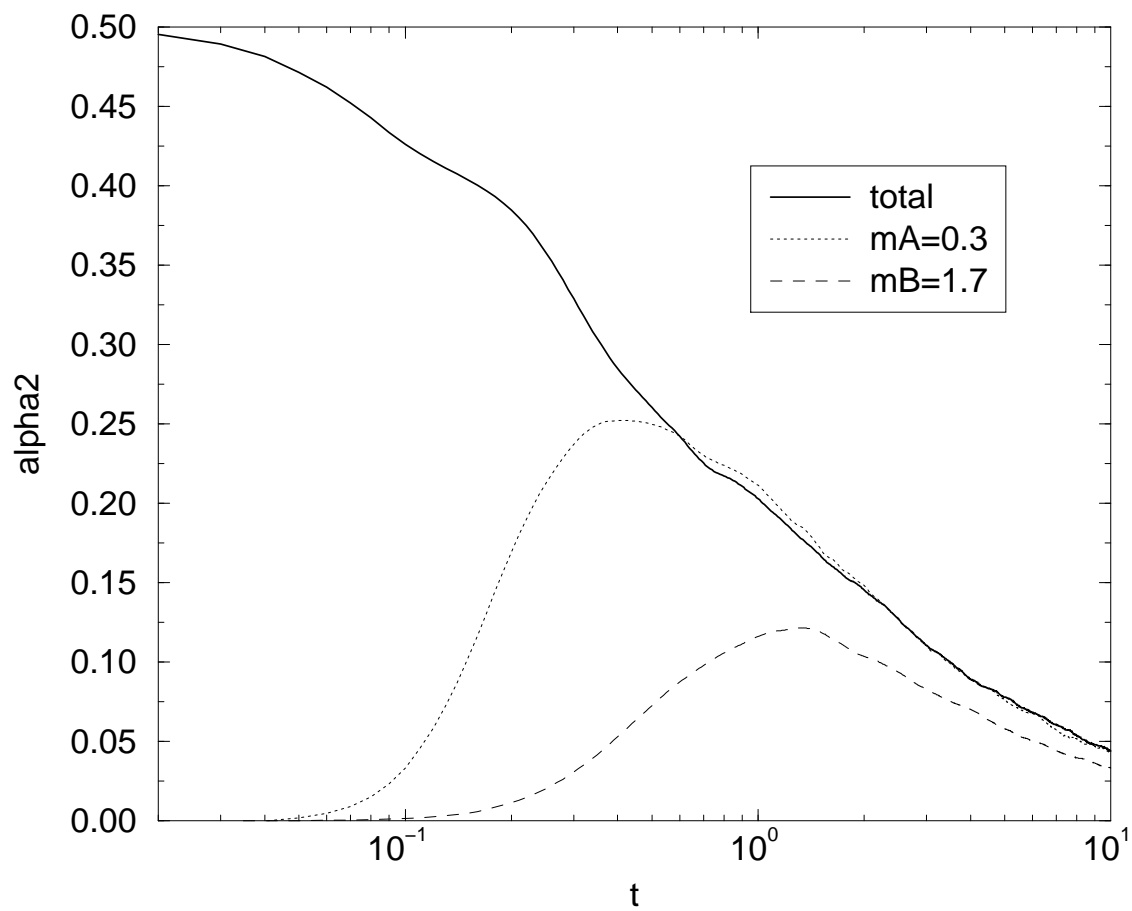


FIG. 8: $\alpha_2(t)$ for lighter, heavier particles, and the total for $\Delta m = 0.7$.

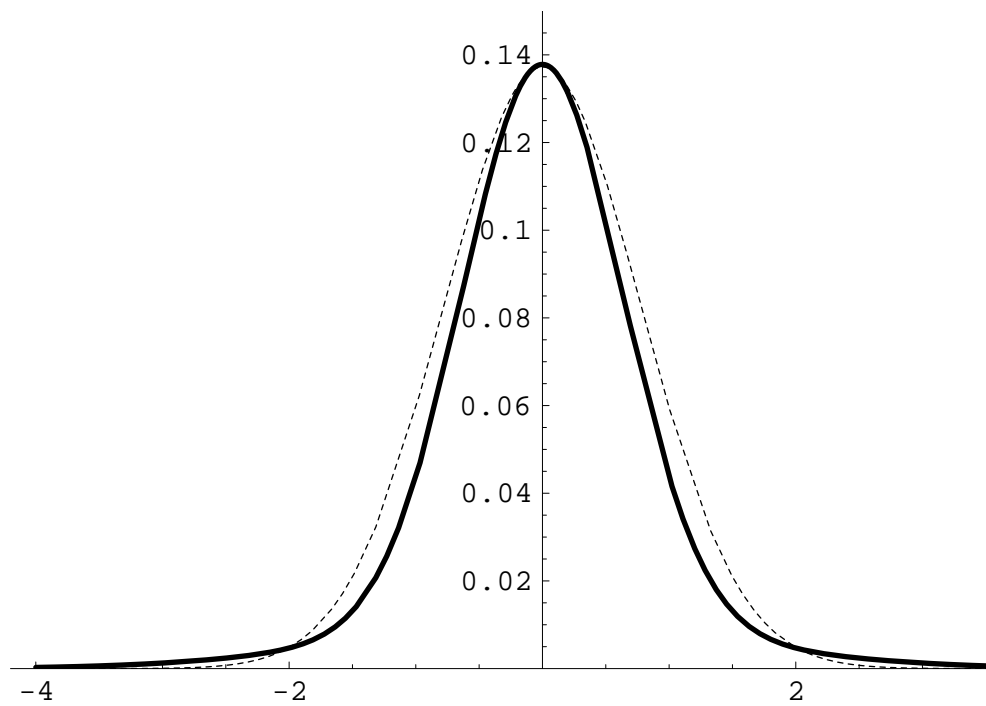


FIG. 9: Distribution of velocities of particles (solid line) and the Gaussian fit (dashed line) for $\Delta m = 0.7$.

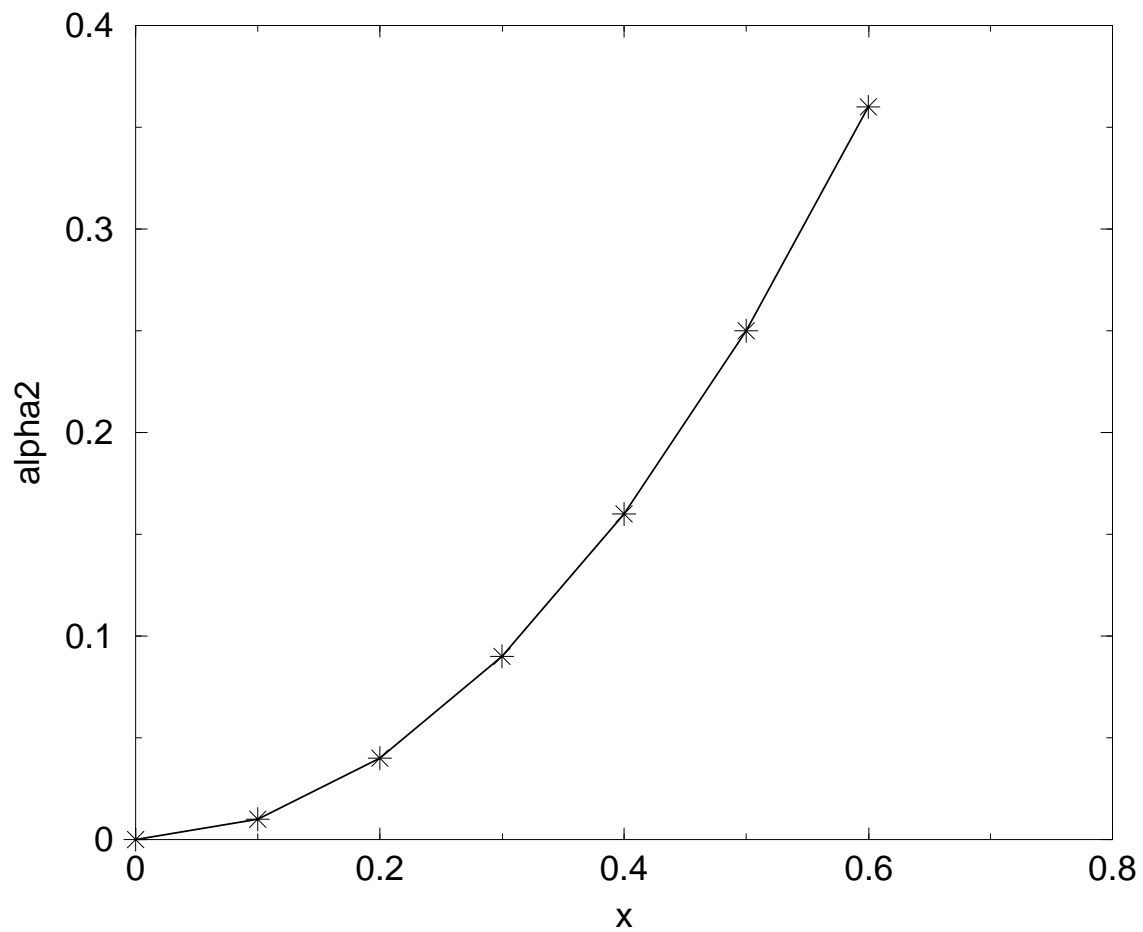


FIG. 10: α_2 versus $x = \Delta m/m_0$. Stars represent results of computer simulation and the solid line is Eq. 13.

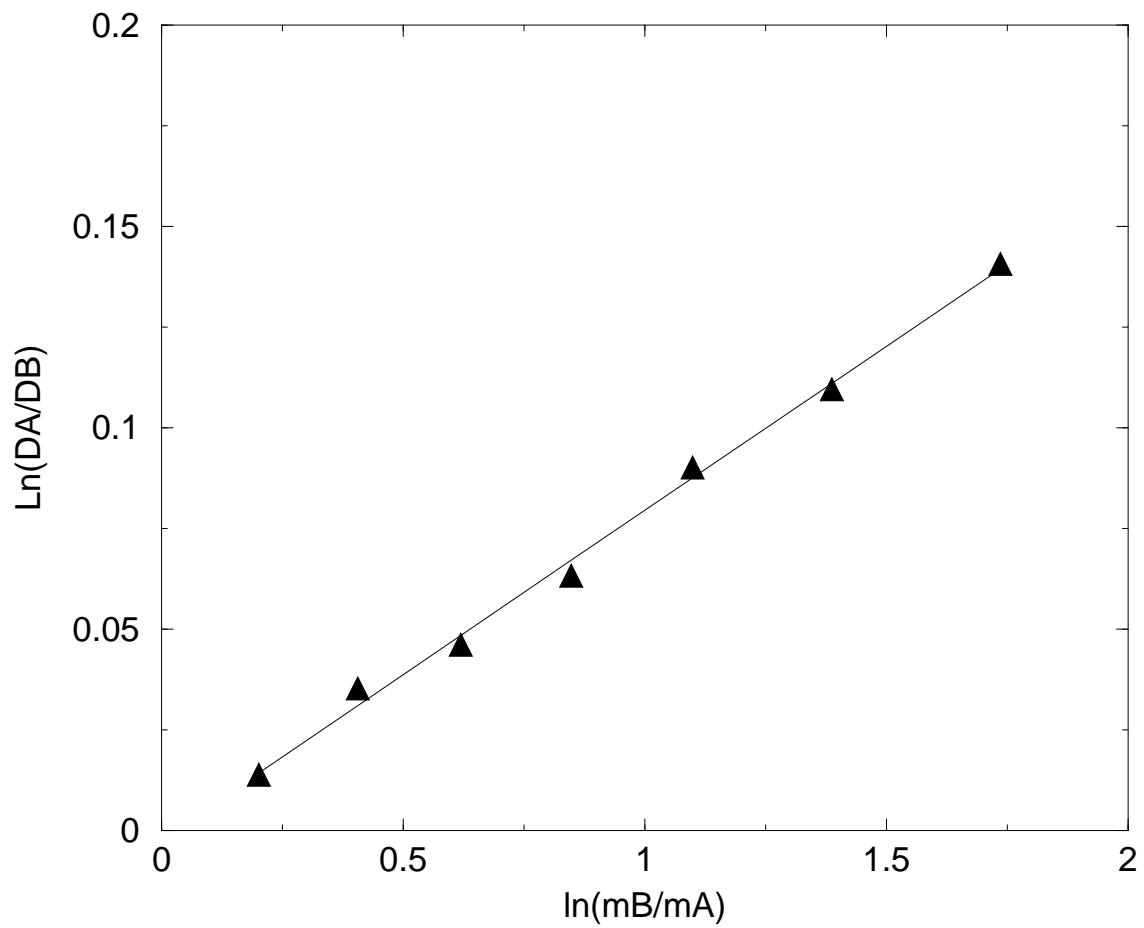


FIG. 11: $\ln(D_A/D_B)$ versus $\ln(m_B/m_A)$. Triangles are results of computer simulation and the solid line is the best fit line. γ is the slope of this line.